Squier, T. C., Bigelow, D. J., & Thomas, D. D. (1988a) *J. Biol. Chem. 263*, 9178.
Squier, T. C., Hughes, S. E., & Thomas, D. D. (1988b) *J. Biol. Chem. 263*, 9162.
Taylor, K., Dux, L., & Martonosi, A. (1984) *J. Mol. Biol. 174*, 193.
Thomas, D. D. (1986) in *Techniques for Analysis of Membrane Proteins* (Ragan, I., & Cherry, R., Eds.) pp 377–431, Chapman & Hall, London.
Thomas, D. D., & Hidalgo, C. (1978) *Proc. Natl. Acad. Sci. U.S.A. 75*, 5488.
Thomas, D. D., Bigelow, D. J., Squier, T. C., & Hidalgo, C. (1982) *Biophys. J. 37*, 217.
Vanderkooi, J. M., Ierokomos, A., Nakamura, H., & Martonosi, A. (1977) *Biochemistry 16*, 1262.
Van Winkle, W. B., Bick, R. J., Tate, C. A., & Entman, M. L. (1985) *Biophys. J. 47*, 284a.
Varga, S., Csermely, P., & Martonosi, A. (1985) *Eur. J. Biochem. 148*, 119.
Volpe, P., Damiani, E., Maurer, A., & Tu, A. T. (1986) *Arch. Biochem. Biophys. 246*, 90.
Wang, T. (1986) *J. Biol. Chem. 261*, 6307.
Watanabe, T., Lewis, D., Nakamoto, R., Kurzmack, M., Fronticelli, C., & Inesi, G. (1981) *Biochemistry 20*, 6617.
Yantorno, R. E., Yamamoto, T., & Tonomura, Y. (1963) *J. Biochem. (Tokyo) 94*, 1137.

# Probing the Relationship between $\alpha$-Helix Formation and Calcium Affinity in Troponin C: $^1$H NMR Studies of Calcium Binding to Synthetic and Variant Site III Helix–Loop–Helix Peptides†

Gary S. Shaw, Robert S. Hodges, and Brian D. Sykes*

*Department of Biochemistry and MRC Group in Protein Structure and Function, University of Alberta, Edmonton, Alberta T6G 2H7, Canada*

*Received March 15, 1991; Revised Manuscript Received May 29, 1991*

ABSTRACT: Three 34-residue peptides corresponding to the high-affinity calcium-binding site III and two variant sequences from the muscle protein troponin C (TnC) were synthesized by solid-phase techniques. The two variant 34-residue peptides had amino acid modifications at either the coordinating positions or both the coordinating and noncoordinating positions, which corresponded to the residues found in the low-affinity calcium-binding site II of TnC. High-field $^1$H NMR spectroscopy was used to monitor calcium binding to each peptide to determine the effect these amino acid substitutions had on calcium affinity. The dissociation constant of the native site III peptide (SCIII) was $3 \times 10^{-6}$ M, smaller than that of the peptide incorporating the ligands from site II (LIIL), $8 \times 10^{-6}$ M, and that with the entire site II loop (LII), $3 \times 10^{-3}$ M, which bound calcium very weakly. These calcium dissociation constants demonstrate that very minor amino acid substitutions have a significant effect on the dissociation constant and give some insight into why the dissociation constants for site III and IV in TnC are 100-fold smaller than those for sites I and II. The results suggest that the differences in coordinating ligands between sites II and III have very little effect on $Ca^{2+}$ affinity and that the noncoordinating residues in the site II loop are responsible for the low affinity of site II compared to the high affinity of site III in TnC.

Calcium-binding proteins comprise a large class of regulatory proteins that contain between one and four highly conserved metal-ion binding sites. In many cases the trademark of these calcium-binding sites is a contiguous sequence of about 30 amino acids that forms a helix–loop–helix structural motif upon binding of calcium (Kretsinger & Nockolds, 1973). Coordination of the metal ion in these proteins occurs in a 12-residue loop region where calcium is ligated to the carboxyl, amide, or hydroxyl side chains of five amino acid residues at positions 1 (X), 3 (Y), 5 (Z), 9 (−X), and 12 (−Z) and to the main-chain carbonyl of the residue at position 7 (−Y). These residues form a pentagonal bipyramid arrangement about the calcium ion in which the carboxylate side chain of the residue at position −Z chelates the metal in a bidentate fashion (Strynadka & James, 1989).

Recently, a detailed analysis of all available amino acid sequences for calcium-binding proteins that have contiguous calcium-binding loops was compiled in an effort to determine a preference for amino acids at various positions of the loop (Marsden et al., 1990). It was found that for the 12 loop positions the only invariant amino acids existed at positions 1, 6, and 12 where aspartic acid, glycine, and glutamic acid residues, respectively, are highly favored (>85%). As the calcium affinity of a calcium-binding protein is most likely a function of the composition of the calcium-binding loop, the variability of the nine positions in the calcium-binding loops is consistent with the dramatic range of calcium affinities within the family of calcium-binding proteins. For example, parvalbumin has one of the highest measured calcium affinities [$K_d \approx 10^{-9}$ M, Goodman et al. (1979)] while some aequorin proteins can have a calcium affinity that is several orders of

† This study was supported by a research grant from the Medical Research Council of Canada and an Alberta Heritage Foundation for Medical Research Fellowship (G.S.S.).
* Author to whom correspondence should be addressed.

0006-2960/91/0430-8339$02.50/0 

magnitude lower [$K_d \approx 10^{-2}$ M, Allen et al. (1977)]. This variability also applies for calcium-binding sites within a single protein. The muscle protein troponin C (TnC)[1] has two distinct classes of calcium-binding sites (Potter & Gergely, 1975); two high-affinity sites (III and IV) in the C-terminal domain ($K_d = 5.0 \times 10^{-8}$ M), which also bind magnesium ($K_d = 2.0 \times 10^{-4}$ M), and two lower affinity sites (I and II) in the N-terminal domain ($K_d = 2.0 \times 10^{-6}$ M).

One technique for analyzing the relative contribution of a particular amino acid to metal-ion binding is site-specific mutagenesis and the production of variant proteins. This approach has been used successfully by several groups to study the importance of the coordinating residues for calcium binding. In oncomodulin, several residues in the CD calcium-binding loop have been replaced with the corresponding residues found in rat parvalbumin (MacManus et al., 1989; Hapak et al., 1989; Golden et al., 1989; Palmisano et al., 1990). Substitutions at positions 52 (Y), 54 (Z), and 57 were found to have little effect on calcium affinity (Palmisano et al., 1990). However, substitutions at positions 59 (−X) and 60 had a marked effect, and the double variant protein (D59E/G50E) had an increased affinity compared to the wild-type protein. Similarly in cardiac TnC several substitutions were made in the inactive site I in order to convert it to an active calcium-binding site (Putkey et al., 1989). Further, calcium-binding site II was rendered inactive by converting the aspartic acid residue at position X to an alanine. In calbindin $D_{9k}$, which has two calcium-binding loops, a number of studies have shown the importance of electrostatic interactions between calcium-binding loops (Linse et al., 1987, 1988; Hofmann et al., 1988). In particular, it has been found that amino acid replacement in site I can have a dramatic effect on the calcium-binding properties of both sites. These approaches have also been extended to other calcium-binding proteins such as staphylococcal nuclease (Serpersu et al., 1987) and subtilisin (Pantoliano et al., 1988, 1989), which do not have contiguous calcium-binding loops.

The contiguous nature of the calcium-binding sites in many calcium-binding proteins has allowed their metal-ion binding properties to be studied by using synthetic peptides (Reid et al., 1981; Gariépy et al., 1982; Reid, 1987; Borin et al., 1985, 1989; Buchta et al., 1986; Malik et al., 1987; Kanellis et al., 1983; Marsden et al., 1988; Marchiori et al., 1983) and protein fragments (Drabikowski et al., 1982; Leavis et al., 1978; Nagy et al., 1978). Calcium binding to a series of peptides derived from site III of TnC has been studied by Reid et al. (1981), who found that a 34-residue peptide was required for relatively tight calcium binding ($K_d \approx 3.8 \times 10^{-6}$ M). Shorter peptides had decreased calcium affinity, and the isolated 12-residue calcium-binding loop binds calcium very weakly ($K_d \approx 10^{-3}$ M). While the length of the peptide is important for calcium binding, the amino acid composition of the calcium-binding loop also appears to have an important contribution. This has recently been probed by Marsden et al. (1988) using a series of synthetic 13-residue peptides representing all possible permutations of Asp and Asn in the X, Y, and Z coordinating positions. The most favorable combination judged from the lanthanum binding studies was Asp (X), Asn (Y), Asp (Z). Interestingly, this same combination is found in all known sequences for the high-affinity sites III and IV of TnC but does not occur in the low-affinity sites I and II (Marsden et al., 1990).

Table I: Calcium Dissociation Constants for the 34-Residue Site III Helix–Loop–Helix Peptides

| peptide[a] | calcium binding loop sequence[b] 1 X | 3 Y | 5 Z | 7 −Y | 9 −X | 12 −Z | dissociation constant (M) |
|---|---|---|---|---|---|---|---|
| | 106 | | | | | 117 | |
| SCIII | **D**-K-**N**-A-**D**-G-**Y**-I-**D**-I-**E**-**E** | | | | | | $3 \times 10^{-6}$ |
| LIIL[c] | **D**-K-D-A-S-G-T-I-**D**-I-**E**-**E** | | | | | | $8 \times 10^{-6}$ |
| LII | **D**-E-D-G-S-G-T-I-**D**-F-E-**E** | | | | | | $3 \times 10^{-3}$ |

[a] The three 34-residue helix–loop–helix peptides varied only in the 12-residue loop region as shown above, and each contained the same N-terminal [Ac TnC (93–105); Ac-K-S-E-E-E-L-A-N-A-F-R-I-F-] and C-terminal [TnC (118–126)-amide; L-G-E-I-L-R-A-T-G-amide] sequence. Ac = acetyl. [b] Calcium-coordinating residues are indicated in bold and their positions in the calcium-binding loop are indicated numerically and according to an octahedral arrangement of the ligands (Kretsinger & Nockolds, 1973). [c] Underlined residues denote amino acid changes from the native sequence SCIII.

In this work we have used a synthetic peptide approach in an effort to understand the reasons for the difference in affinities between the two classes of calcium-binding sites in TnC. We describe the synthesis and calcium-binding properties of three synthetic helix–loop–helix peptides derived from sites II and III of chicken skeletal troponin C and have focused on the contributions that the coordinating and noncoordinating residues in the $Ca^{2+}$-binding loop make toward calcium affinity. This was accomplished by replacing the ligands from site III with those found in site II or by incorporating the entire calcium-binding loop from site II into the site III helix–loop–helix. The calcium affinity of each of these peptides was determined by calcium titration experiments monitored by high-field $^1$H NMR spectroscopy and compared to that for native site III of TnC.

## Experimental Procedures

*Materials.* Co-polystyrene (1% divinylbenzene) benzhydrylamine hydrochloride (BHA) resin was purchased from Institut Armand Frappier (Laval, Quebec, Canada). Protected amino acid derivatives were purchased either from Institut Armand Frappier or Bachem Fine Chemicals (Torrance, CA). Deuterated imidazole was obtained from MSD Isotopes (Montreal, Quebec, Canada). Puratronic grade calcium chloride (99.9975%) was obtained from Alfa Chemical Products (Danvers, MA). All other materials were those as described by Hodges et al. (1988).

*Synthesis of STnC (93–126) Helix–Loop–Helix Peptides.* The peptides were synthesized according to the general procedures for stepwise solid-phase synthesis of Hodges et al. (1981, 1988). Amino acids were protected at the $\alpha$-amino position with a Boc group, and the following side chain protecting groups were used: benzyl (Thr, Ser), *p*-toluenesulphonyl (Arg), benzyl ester (Glu, Asp), 2-bromobenzyloxycarbonyl (Tyr), and 2-chlorobenzyloxycarbonyl (Lys). The C-terminal residue, Gly 126, was coupled to the BHA resin (2 mmol) to obtain a neutral C-terminal amide on each peptide after cleavage of the peptide from the solid support. The next 10 residues were double coupled, except for the glutamic acid residues, which were triple coupled, with a Beckman peptide synthesizer (model 990). Each coupling was monitored with ninhydrin to insure that coupling efficiencies were ≥99.5%.

The peptide resin, containing the first 11 residues, was then

[1] ICP analysis, inductive coupled plasma spectroscopy; TnC, troponin C; E-helix, residues 93–105 of TnC; F-helix, residues 115–126 of TnC; G-helix, residues 131–141 of TnC, H-helix, residues 151–162 of TnC; site III, residues 93–126 of TnC; site IV, residues 129–162 of TnC; Boc, *tert*-butyloxycarbonyl; HOBt, 1-hydroxybenzotriazole; DSS, 4,4-dimethyl-4-sila-1-pentanesulfonate, sodium salt.

divided into four portions. The synthesis was continued on an Applied Biosystems peptide synthesizer (model 430A) using three aliquots (0.5 mmole each) of the peptide resin and adding the next 10 residues corresponding to each of the calcium-binding "loops" of SCIII, LII, and LIIL (Table I). During this stage of each synthesis, each protected amino acid was double coupled as the preformed symmetric anhydride (except Asn and Arg, which were coupled as the HOBt active ester). One-third of each of the 21-residue peptide resins (0.16 mmole) was then sealed in a 2.5 cm × 3.5 cm polypropylene bag and the three "tea-bags" placed in the 0.5 mmol reaction vessel of the Applied Biosystems peptide synthesizer for simultaneous synthesis. The remaining 13 residues were then double coupled as described immediately above, except for Arg 103, which was manually coupled a third time for 1 h. The peptides were acetylated following the coupling of the final residue by using 25% acetic anhydride/dichloromethane. Each peptide resin was removed from the "tea-bag" and cleaved by treatment with hydrofluoric acid (20 mL/g resin) containing 10% anisole and 2% dithioethanol (Hodges et al., 1988).

*Peptide Purification.* The crude peptides were analyzed and purified on a Varian 5000 Liquid Chromatography System, utilizing a Waters M-490 variable programmable detector. Analytical runs were carried out with an Aquapore RP-300 $C_8$ column (220 × 4.6 mm i.d., 7-μm particle size, 300-Å pore size, Brownless Labs, Santa Clara, CA) at a flow rate of 1 mL/min. An AB gradient was used where eluent A was 0.05% aqueous TFA and eluent B was 0.05% TFA/$CH_3CN$. The retention time of the crude peptide, when a linear A/B gradient was used (1% B/min), was about 46 min. Purification of the three 34-residue peptides was accomplished by using a semipreparative SynChropak RP-P (Linden, IN.) reverse-phase $C_{18}$ column (250 mm × 10 mm i.d.) at a flow rate of 2.0 mL/min. The peptide (40–60 mg) was dissolved in about 4 mL of 50% TFA and centrifuged to remove suspended matter, and the supernatant was injected onto the column. The gradient used was time 0, 100% A; linear gradient to 72% A/28% B (1% B/min for 28 min.); linear gradient to 60% A/40% B (0.1% B/min for 120 min) followed by a rapid gradient to 100% B (7.5% B/min for 8 min). Fractions from each purification run were analyzed on the same instruments as above coupled to a Waters WISP 710 autoinjector system, and the fractions containing a single peak were pooled.

Amino acid analyses of the purified peptides were performed on a Durrum D-500 amino acid analyzer. Each peptide was hydrolyzed with 100 μL of 6 N HCL containing 0.1% phenol in sealed tubes at 110 °C for 24 h. The amino acid analysis of each peptide was consistent with the sequence. Peptides were analyzed by plasma desorption mass spectroscopy using a BioIon-20 mass spectrometer for average chemical mass: SCIII, expected 3870.3, found 3871.0; LIIL, expected 3781.2, found 3780.6; and LII, expected 3802.1, found 3802.0.

*Preparation of Apopeptides for $^1H$ NMR Experiments.* Solutions of each peptide were prepared in about 1 mL of $D_2O$ containing 50 mM KCl and 30 mM imidazole-$d_4$. Residual metal ions were removed by a heated Chelex treatment (Williams et al., 1986). Chelex-100 (Na form) was equilibrated with KCl, washed several times with $D_2O$, and filtered by using a sintered glass funnel. A suspension of Chelex in $D_2O$ (1 g/3 mL) was prepared. A typical Chelex treatment consisted of adding 200–400 μL of filtered Chelex to the peptide solution and heating the suspension for 45 min at 63 °C. The suspension was drawn up in an Eppendorf syringe and filtered through a Millipore 0.45-μm filter to remove the Chelex. Calcium analysis by either inductively coupled plasma spectroscopy (ICP) or back extrapolation of $^1H$ NMR titration data showed that the residual calcium content of any of the peptide solutions was <10 μM. Prior to calcium titrations, aliquots (3 × 10 μL) were removed from each peptide solution and the peptide concentrations determined by amino acid analysis as above, except that hydrolysis was done for 60 min at 160 °C. Concentrations were determined by comparison of the alanine and leucine peak areas with those from a standard 8 nmol sample.

*$^1H$ NMR Experiments.* All calcium titrations were monitored at 30 °C by $^1H$ NMR using a Varian VXR-500 spectrometer. Apopeptide concentrations used were SCIII, 431 ± 6 μM; LII, 451 ± 5 μM; and LIIL, 228 ± 17 μM in sample volumes of 600 μL of buffer, described above. Typical $^1H$ NMR acquisition parameters were spectral width = 5200 Hz, number of transients = 256 or 512, pulse width = 15 μs (90°), and acquisition time = 2 s. Water suppression was accomplished with a 2.0-s presaturation pulse. All spectra were referenced to the trimethylsilyl resonance of DSS (internal) at 0.00 ppm. All data were zero filled to 64K and processed with line broadening of 0.5 Hz.

*Calcium Titration Experiments.* Calcium titrations were monitored at pH 7.35 (SCIII), 7.37 (LIIL), and 7.28 (LII) (uncorrected) by $^1H$ NMR spectroscopy after each successive addition of calcium. Titrations were completed in duplicate for SCIII and LIIL but only once for LII. Calcium stock solutions (10.3 and 102.9 mM) were prepared from $CaCl_2$ dissolved in $D_2O$ and containing 50 mM KCl and 30 mM imidazole-$d_4$. The calcium content was determined by EDTA titration with murexide as the indicator or by ICP analysis. An analysis of the resulting spectra showed that the binding of calcium to peptides SCIII and LIIL occurred in the NMR slow-exchange regime. At each calcium concentration, several resonances throughout the spectrum corresponding to the calcium-saturated form of the peptides were measured and plotted as a function of the calcium to peptide ratio. These curves were "normalized" (Marsden et al., 1988) to arrive at an average curve. Calcium binding to LII was a fast-exchange process, so the change in chemical shift was monitored at each calcium concentration. As the chemical shift changes were very small, each spectrum was corrected for any small differences in temperature (<1 °C). The chemical shift of a particular resonance was accurately determined with a curve-fitting routine for Varian software written by Robert Boyko of the University of Alberta.

Calcium dissociation constants for the peptides were calculated by using the average curves of Ca/peptide vs "normalized" integral or chemical shift change and eq 1, where

$$P + Ca \overset{K_1}{\rightleftharpoons} P^*Ca + P \overset{K_d}{\rightleftharpoons} P^*_2Ca + Ca \overset{K_2}{\rightleftharpoons} P^*_2Ca_2 \quad (1)$$

P represents the unstructured apopeptide, P*Ca is the 1:1 peptide–metal complex, $P^*_2Ca$ is a folded 2:1 peptide–metal complex, and $P^*_2Ca_2$ is the metal-bound peptide dimer. Details for the determination of this mechanism as well as the individual calcium binding constants ($K_1$, $K_2$) and dimerization constant ($K_d$) are provided in a separate publication (Shaw et al., 1991) and are based on the observation that the calcium-bound form of SCIII is a dimer (Shaw et al., 1990).

In the limiting case where $K_d \gg K_1$, eq 1 simplifies to the 1:1 peptide–metal equilibrium (eq 2) where P, Ca, and P*Ca are the unstructured peptide, metal, and folded peptide–metal complex (Williams et al., 1985; Marsden et al., 1988). In this work, only the calcium dissociation constant $K_1$ is considered.

$$P + Ca \overset{K_1}{\rightleftharpoons} P^*Ca \quad (2)$$

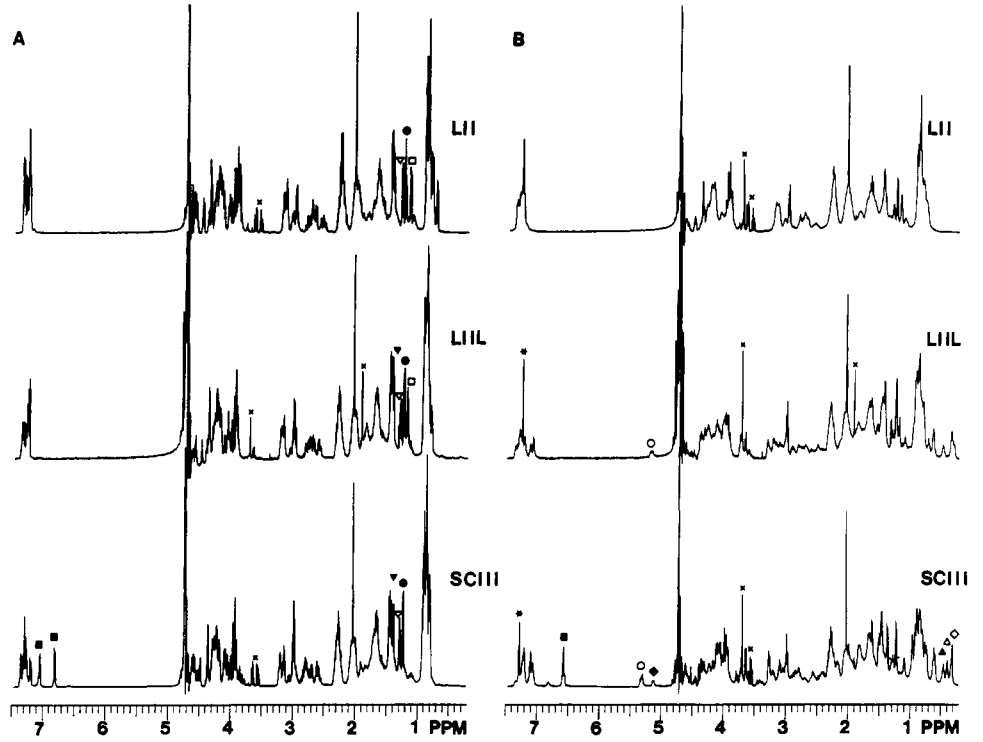


FIGURE 1: 500-MHz $^1$H NMR spectra of SCIII, LIIL, and LII in the apo (A) and calcium-bound (B) forms. The peptide concentrations were 431 $\mu$M SCIII, 451 $\mu$M LIIL, and 228 $\mu$M LII. Calcium-bound forms of the peptides (B) represent spectra where Ca/peptide is approximately 1:1. Resonances for the apopeptides (A) are marked as follows: Y112 $\delta$, $\epsilon$CH (■) in SCIII, A109 $\beta CH_3$ (▼) in SCIII and LIIL, A101 $\beta CH_3$ (▽) and T125 $\gamma CH_3$ (●) in all, and T112 $\gamma CH_3$ (□) in LIIL and LII. In the calcium-bound forms of the peptides (B), the following resonances are marked: Y112, $\delta$, $\epsilon$CH (■), I121 $\delta CH_3$ (▲), I121 $\gamma CH_3$ (◇), I113 $\delta CH_3$ (△), and Y112 $\alpha$CH (◆) in SCIII and I113 $\alpha$CH and D114 $\alpha$CH (○) in SCIII and LIIL. Assignments were made as described in the text. The resonance marked (*) results from the 4,5-protons of the imidazole ring in the buffer, and resonances marked (x) are nonpeptide impurities in the samples. The vertical scales for the apopeptides (A) were adjusted for concentration. For the calcium-bound spectra (B), the vertical scale for LII is identical with that in panel A, and those for SCIII and LIIL were increased to give the same apparent concentration. Conditions are described under Experimental Procedures.

## RESULTS

*Apopeptide $^1$H NMR Spectra.* The peptides selected for this study are all modifications of the site III helix–loop–helix from chicken troponin C extending from residue 93 to 126 (Table I). The native peptide (SCIII) contains a few modifications from the native sequence of chicken TnC at positions 100, 101, and 112. An Asn residue at position 100 has replaced the original Asp residue on the basis of the results of recent DNA sequencing of the chicken TnC gene (Reinach & Karlsson, 1988). We replaced the Cys residue normally found at position 101 by Ala to eliminate the possibility of oxidation and disulfide formation between two peptides, forming a covalently linked dimer. An internal disulfide bond has been shown to occur in TnC by Tsuda et al. (1988) and also in this peptide derivative when Cys is placed at position 101.[2] The Phe residue at position 112 was replaced by Tyr in SCIII to distinguish that residue from the two other Phe residues by $^1$H NMR, since position 112 is one of the ligating positions.

Peptides LIIL and LII are comprised of the helices from site III and thus are identical with peptide SCIII in these regions. The loop of the LIIL peptide contains the six coordinating ligands corresponding to those of low-affinity calcium-binding site II, whereas the LII peptide contains the entire loop, ligands and nonligands, from site II (Table I). A close examination of these sequences reveals that there are only three amino acid residues different between SCIII and LIIL and only a further three-residue difference between LIIL and LII. As a result, the high-resolution $^1$H NMR spectra of these peptides in their apo forms (Figure 1A) are all very similar and several resonance assignments can be made on the basis of the presence or absence of $^1$H resonances when any two spectra are compared. For example, a comparison of the spectra for apo-SCIII with either apo-LIIL or apo-LII allowed the $\delta$CH and $\epsilon$CH resonances of Y112 (SCIII) to be assigned at 7.05 and 6.81 ppm, respectively. Similarly, the $\beta CH_3$ resonance of A109 at 1.40 ppm in apo-SCIII and apo-LIIL was assigned by comparison of these spectra with that for apo-LII, which has glycine at this position. Assignments were also made for T112 $\gamma CH_3$ (1.17 ppm for apo-LII and apo-LIIL) and T125 $\gamma CH_3$ (1.24 ppm for all). One further assignment, A101 $\beta CH_3$ at 1.29 ppm in all of the apopeptides, was made by comparison of the $^1$H NMR spectra with a 34-residue site III peptide that contained C101 in the reduced state.[2]

*Calcium-Induced Changes in $^1$H NMR Spectra.* The addition of calcium to peptides SCIII, LIIL and LII resulted in several significant changes in the $^1$H NMR spectra (Figure 1B) indicative of calcium binding to the peptides and a conformational change. In the case of peptides SCIII and LIIL, several new resonances appear in the presence of calcium that were not present in the apopeptide spectra. As the $^1$H NMR spectrum for calcium-bound SCIII has been completely assigned,[3] some qualitative comments can be made about the nature of the resonances that are affected by the addition of calcium to peptides SCIII or LIIL. The most notable differences are the shifting of several resonances to higher field in the calcium-bound forms of SCIII and LIIL. In SCIII,

[2] C. M. Slupsky, unpublished results.

[3] G. S. Shaw, unpublished results.

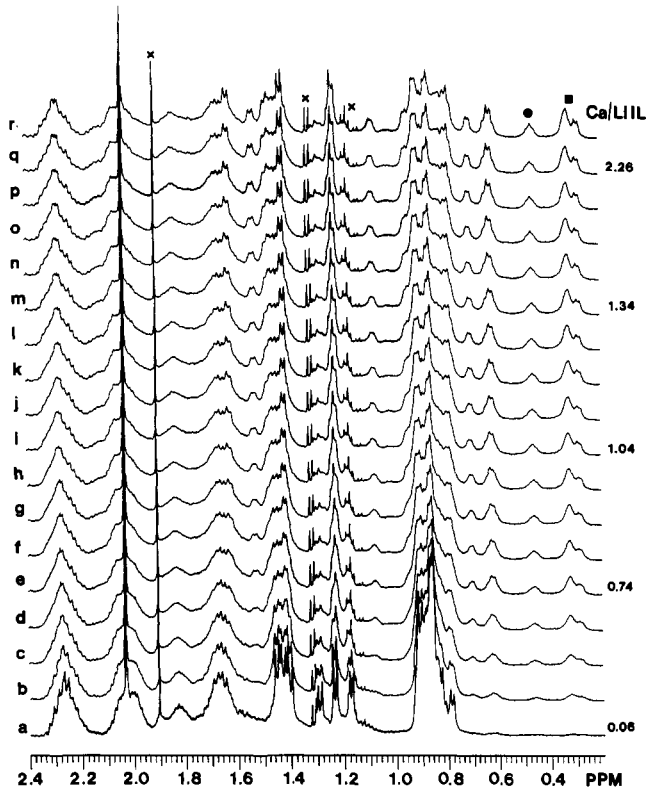


FIGURE 2: 500-MHz $^1$H NMR spectra for 228 $\mu$M LIIL showing a portion of the aliphatic region at the following Ca/peptide ratios: (a) 0.06, (b) 0.29, (c) 0.44, (d) 0.59, (e) 0.74, (f) 0.81, (g) 0.89, (h) 0.96, (i) 1.04, (j) 1.11, (k) 1.19, (l) 1.26, (m) 1.34, (n), 1.42, (o) 1.57, (p) 1.80, (q), and 2.26 (r) 3.02. Some specific ratios (Ca/LIIL) are highlighted on the right side of the figure. Resonances marked with an x are impurities in the sample. The regions marked (■) and (●) were used for calcium titration plots in Figure 4. Conditions are described under Experimental Procedures.

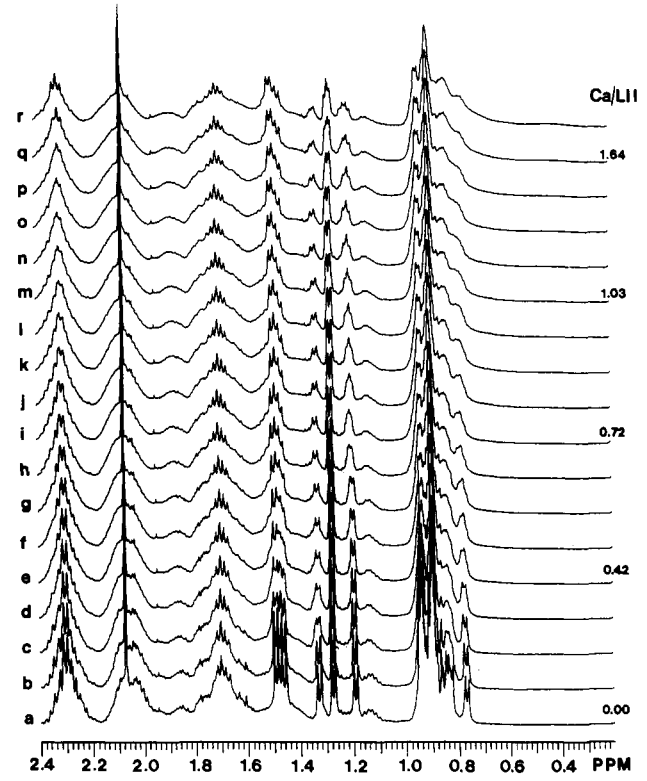


FIGURE 3: 500-MHz $^1$H NMR spectra for 451 $\mu$M LII showing a portion of the aliphatic at the following Ca/peptide ratios: (a) 0.00, (b) 0.11, (c) 0.23, (d) 0.34, (e) 0.42, (f) 0.50, (g), 0.57, (h) 0.65, (i) 0.72, (j) 0.80, (k) 0.88, (l) 0.95, (m) 1.03, (n) 1.10, (o) 1.18, (p) 1.26, (q) 1.64, and (r) 2.41. Some specific ratios (Ca/LII) are highlighted on the right side of the figure. Resonances marked with an x are impurities in the sample. Conditions are described under Experimental Procedures.

these resonances correspond to I121 $\delta CH_3$ (0.45 ppm) and $\gamma CH_3$ (0.36 ppm) and I113 $\delta CH_3$ (0.40 ppm) (Figure 1B). The $^1$H NMR spectra for SCIII and LIIL in the presence of calcium also contain new $\alpha$CH resonances at lower field than the residual HDO signal. These have been assigned to Y112 $\alpha$CH at 5.16 ppm and I113 $\alpha$CH and D114 $\alpha$CH at 5.30 ppm in SCIII (Shaw et al., 1990). By comparison, these resonances likely correspond to I113 $\alpha$CH and D114 $\alpha$CH, both at 5.16 ppm in LIIL. The resonance for T112 $\alpha$CH (LIIL) would be expected to be shifted at least 0.25 ppm upfield of that for Y112 $\alpha$CH (5.16 ppm, SCIII) on the basis of their chemical shift differences in random-coil peptides (Bundi & Wuthrich, 1979) and thus does not clearly appear downfield of the HDO signal.

The spectral changes for LII were not as dramatic as those for SCIII and LIIL upon addition of calcium. Whereas the $^1$H NMR spectra of SCIII and LIIL exhibited several new resonances and large chemical shift changes, the spectrum of peptide LII showed only small changes in chemical shifts while most resonances simply broadened as calcium was added (Figure 1B).

*Calcium Dissociation Constants.* The calcium dissociation constants for SCIII, LIIL, and LII were determined from the $^1$H NMR spectra at many Ca/peptide ratios. These are shown during the course of the calcium titrations for peptides LIIL and LII in Figures 2 and 3, respectively. For LIIL, many new resonances from the calcium-bound species appear throughout the spectrum and are indicated on the figure. Several of these resonances were integrated and plotted as a function of the Ca/LIIL ratio (Figure 4). The $^1$H NMR spectra (Figure 2)

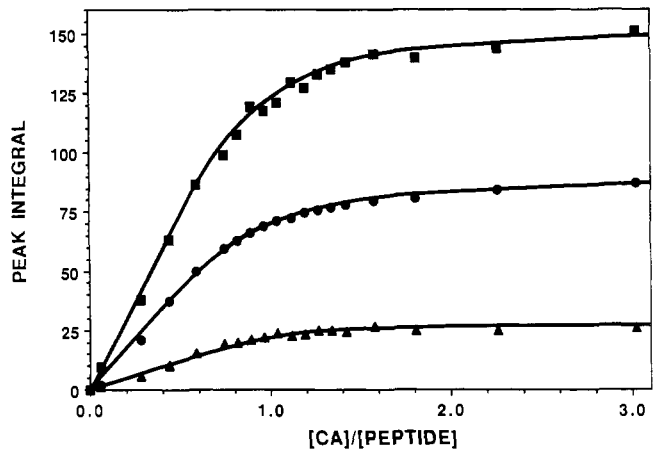


FIGURE 4: Calcium titration plot for 228 $\mu$M LIIL derived from the $^1$H NMR titration data in Figure 2. The curves marked (■) and (●) represent the regions shown in Figure 2 that were integrated at each calcium concentration and plotted as the raw peak integral vs [Ca]/[peptide]. The curve marked (▲) is similarly derived from the I113 $\alpha$CH and D114 $\alpha$CH resonance, marked (○) in Figure 1 (not shown in Figure 2), at each calcium concentration.

and the resulting plot (Figure 4) both show that the resonances for calcium-bound LIIL increase in area until a Ca/LIIL ratio of $\approx$1:1 is reached. This indicates that the stoichiometry is one calcium ion to one molecule of LIIL and that the peptide has a relatively high affinity for the metal.

Calcium binding to LII was considerably more difficult to measure than for either SCIII or LIIL due to the extensive broadening of the resonances as the calcium concentration was increased (Figure 3). However, close examination of the

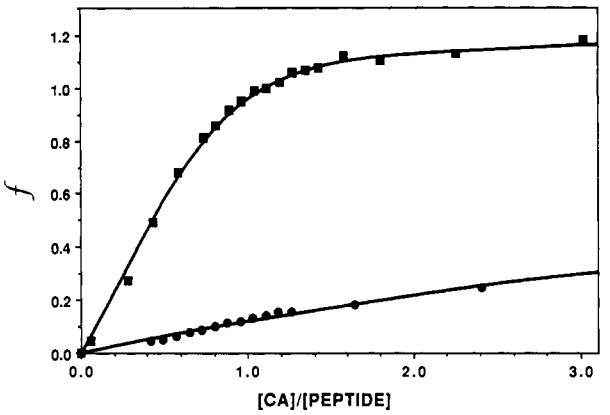


FIGURE 5: Calcium titration plot for 228 μM LIIL (■) derived from Figure 4. Peak integrals from Figure 2 were normalized from the peak integral at 1:1 [Ca]/[peptide] and averaged to obtain the normalized average integral *f*, which was plotted vs [Ca]/[peptide]. The curve shown is the best fit line through the points corresponding to a dissociation constant of $8 \times 10^{-6}$ M. Also shown is the calcium titration plot for 451 μm LII (●). The normalized average integral *f* was calculated on the basis of the observed change in chemical shift and a calculated maximum shift (65.4 Hz) at infinite [Ca]/[peptide]. At low [Ca]/[peptide], chemical shift changes in LII were very small (<0.5 Hz) and could only be measured once a particular resonance in the spectrum was completely resolved from other peaks.

spectra revealed that some resonances underwent small chemical shift changes, similar to those observed for lanthanum binding studies to calcium-binding loop peptides (Marsden et al., 1988). Typically these chemical shift changes represented <0.5 Hz at the outset of the calcium titration (<1:1 Ca/peptide) where the calcium additions were about 50 μM Ca/addition (~0.11 Ca/peptide). These were measured in a similar manner as done by Marsden et al. (1988) in order to obtain a calcium dissociation constant for LII.

The interaction of calcium with each peptide is described by eqs 1 and 2 under Experimental Procedures. In each case several individual resonances were plotted as a function of Ca/peptide, normalized for maximal change and averaged to determine an average curve. The normalized value *f* was then plotted vs Ca/peptide (Figure 5). For peptide SCIII, calcium binding also resulted in peptide association (Shaw et al., 1990), which complicated the $^1$H NMR spectral analysis and yielded a stoichiometry of 1:2 Ca/peptide (Shaw et al., 1991). Thus, the dissociation constant for calcium binding to SCIII was calculated by using eq 1 and is presented in this work only for comparison purposes. For peptides LIIL and LII, eq 2 was used to calculate the dissociation constants as both of these peptides displayed 1:1 Ca/peptide stoichiometry. While eq 1 could have been used for the calculation of the dissociation constants for LIIL and LII, the observed stoichiometries for these peptides show that the calcium-binding process is not affected by the peptide association as in SCIII. This represents a limiting case where $K_d \gg K_1$ (eq 2), and use of eq 1 would only allow a lower limit for $K_d$ to be determined. The resulting calcium dissociation constants are presented in Table I.

## Discussion

The three synthetic peptides studied in this work are all 34 residues in length and represent contiguous helix–loop–helix calcium-binding sites. Many other studies have utilized synthetic peptides to monitor the metal-ion binding to calcium-binding sites. However, most of these studies have involved peptides that are much shorter in length (Borin et al., 1985, 1989; Buchta et al., 1986; Malik et al., 1987; Kanellis et al., 1983; Reid et al., 1981; Marsden et al., 1988; Marchiori et al., 1983; Tsuji & Kaiser, 1991). As a result, the calcium affinities of many of these peptide analogues are extremely low, prompting the use of calcium mimics from the lanthanide series, having a higher atomic charge and therefore a greater electrostatic interaction with the peptide. Previously, it has been shown that a 34-residue helix–loop–helix peptide is capable of binding calcium (Reid et al., 1981), so this length of peptide was chosen for calcium-binding studies here. The amino acid sequences of the three peptide analogues are shown in Table I. In order to simplify the study, the helices on either end of the 12-residue calcium-binding loop were not modified so that contributions from these residues should remain constant for all three peptides. Thus the native site III peptide (SCIII) is comprised of the helix–loop–helix sequence from the high-affinity site III of TnC, peptide LIIL has the coordinating residues of peptide SCIII replaced by those found in the low-affinity site II, and peptide LII has the entire calcium-binding loop of SCIII replaced by that found in site II. In this manner, the three analogues studied here probe the residues that are expected to be the most important for the higher affinity of site III in TnC compared to site II. Unlike previous studies, this work encompasses peptides that have had both the coordinating and noncoordinating positions substituted.

Before discussing the calcium dissociation constants for peptides SCIII, LIIL, and LII, it is informative to assess the $^1$H NMR spectral differences between them. The $^1$H NMR spectra of the apopeptides (Figure 1A) are all similar, and the nondispersive nature of the $^1$H resonances and relatively narrow line widths (Figure 1A) indicate that each of these apopeptides has little regular secondary structure (Bundi & Wuthrich, 1979). This is in agreement with circular dichroism studies (Reid et al., 1981), which predict that a 34-residue calcium-binding peptide from TnC contains less than four residues in an α-helical conformation in the absence of metal ion and with the same conclusions reached for other calcium-binding proteins or peptides (Gariepy et al., 1982; Marsden et al., 1988; Drakenberg et al., 1987). In general, the similarity of the $^1$H NMR spectra of the apopeptides also indicates that the amino acid substitutions made in peptides LIIL and LII have little effect on the conformation relative to SCIII.

In the presence of calcium, the $^1$H NMR spectra of peptides SCIII and LIIL at a Ca/peptide ratio of 1:1 (Figure 1B) are very similar and suggest that the calcium-bound forms of these peptides are also similar. Since it has been shown, with two-dimensional $^1$H NMR techniques, that calcium-bound SCIII has a helix–loop–helix conformation (Shaw et al., 1990), it is probable that peptide LIIL also forms the helix–loop–helix motif in the presence of calcium. Assessing the structure of calcium-bound LII is more difficult because the spectral differences between apo- and calcium-bound LII are more subtle at a Ca/peptide ratio of 1:1 (Figure 1B). At higher calcium concentrations, a broad resonance appears at ≈0.4 ppm that may be similar to the resonances observed for SCIII and LIIL in this region (Figure 2). This may indicate that the calcium form of LII is a helix–loop–helix, but, at the Ca/peptide ratios assessed by $^1$H NMR, the proportion of calcium-bound LII is very small. This is consistent with the dissociation constants reported in Table I showing that LII has a weak calcium affinity. It may be possible to "force" the LII–calcium equilibrium (eq 1) further toward the calcium-bound form at higher calcium concentrations in order to make a more definitive statement about its conformation However, since nonspecific binding to calcium-binding loop peptides has previously been observed (Marsden et al., 1988) and this type of binding has been reported to induce helix formation in

peptides (Ghadiri & Choi, 1990), higher calcium concentrations were not pursued.

The calcium titration experiments (Figures 2 and 3) show that the three peptides studied bind calcium over two different chemical exchange time regimes. Calcium titrations of SCIII (Shaw et al., 1991) and LIIL (Figure 2) show that at Ca/peptide ratios <1:1, two distinct sets of resonances are present for the apo- and calcium-bound peptides, typical of NMR slow-exchange kinetics. For calcium-binding peptides and proteins, this is usually an indication of tight calcium binding (Williams et al., 1986; Drakenberg et al., 1987; Corson et al., 1986; Tsuda et al., 1988). In contrast, the $^1$H NMR spectra of peptide LII (Figure 3) display extensive line broadening and chemical shift averaging for the apo- and calcium-bound species. This is representative of intermediate and fast exchange processes, respectively, and usually corresponds to weaker calcium binding.

The calcium dissociation constants for the three peptides are presented in Table I. The native site III peptide, SCIII, exhibited the highest calcium affinity of $3 \times 10^{-6}$ M. This affinity, determined by calcium titration as followed by $^1$H NMR, is similar to a previous measurement by Reid et al. (1981), where a value of $3.8 \times 10^{-6}$ M was found by using circular dichroism. The calcium dissociation constant of SCIII is about 3-fold lower than that measured for LIIL, which has the ligands from site II of TnC. Each of these peptides has a ligand charge of −4 in the loop, although there are three differing residues between the sequences. Peptide SCIII has Asn, Asp, and Tyr residues at metal-coordinating positions Y, Z, and −Y, whereas in LIIL these positions are occupied by Asp, Ser, and Thr residues (Table I). As a result, peptide SCIII has the sequence Asp-Asn-Asp at positions X, Y, and Z of the calcium-binding loop, while peptide LIIL has Asp-Asp-Ser at these positions. These two sequences of the X, Y, and Z coordinating residues have been studied by Marsden et al. (1988) for a series of 13-residue calcium-binding loop peptides. In these latter peptides, the lanthanum affinity was found to be about 10-fold greater for the X, Y, Z sequence Asp-Asn-Asp compared to Asp-Asp-Asn. It has been suggested that negatively charged amino acids at positions X and Y give rise to dentate–dentate electrostatic repulsion and result in this observed decrease in calcium affinity (Reid & Hodges, 1980; Marsden et al., 1988).

While the results for SCIII and LIIL are in qualitative agreement with the 13-residue peptides studied by Marsden et al. (1988), there is some discrepancy between the magnitude of the effect of exchanging ligands in the Y and Z positions on metal-ion affinity. In the 34-residue peptides studied here, the inclusion of the flanking helices seems to dilute the effect of the ligand position on calcium affinity. This suggests that in the shorter 13-residue loop peptides affinity is primarily controlled by the position of charged coordinating residues, whereas in the helix–loop–helix peptides this effect becomes less important. However, on the basis of the small differences in affinity for SCIII and LIIL, it is clear that ligation of the metal ion must be influenced by factors other than the coordinating residues in order to explain the lower affinity of site II compared to site III in TnC.

Peptide LII has the weakest calcium affinity of the three peptides studied (Table I). The calcium dissociation constant, $3 \times 10^{-3}$ M, is approximately 1000-fold higher than that for either peptide LIIL or SCIII. This result is even more significant when one considers that the amino acid substitutions made in LII were at the noncoordinating positions only and represent only three residue modifications compared to LIIL. A rationale for this decrease in affinity in LII can be derived from a residue by residue comparison with peptides SCIII and LIIL. The coordinating residues of peptides LII and LIIL are identical since they are both those from site II of troponin C. Since peptide LIIL had a slightly lower calcium affinity compared to peptide SCIII, a similar result might be expected for peptide LII on the basis of coordinating residues only. This type of analysis has been shown previously for mutant calbindin $D_{9k}$ proteins where the effects of several mutations has been found to be roughly additive with respect to calcium binding (Akke & Forsen, 1990). However, peptide LII has three further substitutions at noncoordinating positions are compared to LIIL. These occur at positions 2 (Lys → Glu), 4 (Ala → Gly), and 10 (Ile → Phe) of the calcium-binding loop (Table I). The modifications at positions 4 and 10 would be considered conservative on the basis of the hydrophobicity (Guy, 1985) and side-chain volumes (Chothia, 1974) of Ala vs Gly and Ile vs Phe. However, the replacement of the basic lysine residue at position 2 of peptide SCIII or LIIL by an acidic glutamic acid in LII is more critical. An examination of all known sequences of troponin C proteins (Marsden et al., 1990) shows that the amino acid which occupies position 2 of the calcium-binding loop of either sites III and IV is an invariant basic residue (lysine or arginine). For sites I and II three different amino acids occupy this location, Glu, Ala, and Thr, in that order of frequency of occurrence. Since the calcium dissociation constants of sites III and IV are approximately 100-fold lower than for sites I and II, the measured dissociation constants obtained here suggest that the Lys/Arg to Glu, Ala, or Thr substitution at position 2 may be partly responsible for this effect.

It has previously been shown by Reid and co-workers (1981) that calcium affinity is dependent on the peptide length. A series of synthetic peptides representing the loop–C-terminal helix (21 residues), partial N-terminal helix–loop–C-terminal helix (26 residues), and entire helix–loop–helix (34 residues) were used to show that affinity increased dramatically as the N-terminal helix (E-helix) was increased in length. More importantly, this study suggested that the induction of the E-helix by calcium binding is a prerequisite for tight calcium binding. The calcium dissociation constants for LII ($3 \times 10^{-3}$ M) and the 21-residue (103–123) peptide ($3.2 \times 10^{-3}$ M) studied by Reid are remarkably similar, despite the fact that LII has residues capable of forming the E-helix. Since the only other major difference between peptide LII and the 21-residue peptide is at position 2 of the calcium-binding loop of LII where lysine has been replaced by glutamic acid, it seems plausible that this residue alone may be perturbing E-helix formation, resulting in a marked decrease in calcium affinity of LII compared to SCIII and LIIL.

The role of the basic residue at position 2 of the calcium-binding loop can be assessed from the architecture of the helix–loop–helix from site III of troponin C. The E-helix spans residues 93–105, while the F-helix is comprised of residues 115–126. Position 2 of the calcium-binding loop for site III is K107 and resides near the C-terminal end of the E-helix. From the crystal structures of TnC (Herzberg & James, 1988; Satyshur et al., 1988), it has been found that the side chain of K107 is exposed to solvent and is directed back toward the E-helix. A similar phenomenon is found for K143 in position 2 of site IV. On the basis of these observations, Strynadka and James (1989) have suggested that this residue acts to stabilize the E-helix through a helix–dipole mechanism.

In general, it has been suggested that an $\alpha$-helix possesses a macroscopic dipole having a partial positive charge at its

N-terminal and a partial negative charge at its C-terminal end (Hol, 1985; Hol et al., 1978, 1981; Shoemaker et al., 1987; Nicholson et al., 1988). It would be expected that a positively charged amino acid at the C-terminal end of helix E for site III (and helix G for site IV) would offer helix stabilization via a helix–dipole mechanism. In the calcium-binding loops of SCIII and LIIL residue K107 at position 2 of the loop carries a positively charged side chain at pH 7.3 (the conditions of this study) the C-terminal end of the E-helix. On the other hand, peptide LII has a negatively charged glutamic acid at position 2. In the presence of calcium, this would act to destabilize $\alpha$-helix formation (E-helix) in peptide LII compared to SCIII and LIIL, resulting in an increased dissociation constant for LII as observed in this study.

An alternative explanation for the decreased calcium affinity of LII compared to SCIII and LIIL may arise from a possible $i$+4 electrostatic interaction, which has been found to stabilize $\alpha$-helices through side-chain salt bridge formation (Marqusee & Baldwin, 1987). X-ray crystallographic studies of skeletal TnC (Herzberg & James, 1988, Satyshur et al., 1988) have revealed that frequent $i$+4 interactions occur in the $\alpha$-helices of this protein. In peptide LII, an excellent $i$+4 arrangement exists between position 103 (Arg) and position 107 (Glu) for helix formation (Table I). A similar $i$+4 arrangement is not possible in peptides SCIII and LIIL as positions 103 and 107 are occupied by Arg and Lys, respectively, in both. It might be expected that promoting an $\alpha$-helix in this region of the calcium-binding site may distort the calcium-binding loop and thus disrupt calcium binding. This effect could be responsible for the decreased calcium affinity of LII compared to SCIII and LIIL.

The data presented in this work show the importance of the noncoordinating residues in the calcium-binding sites of TnC and their roles in calcium binding. On the basis of the sequences of the calcium-binding loops of the low-affinity sites I and II compared to those of the high-affinity sites III and IV, it appears that a basic residue at position 2 of these calcium-binding loops has a dramatic effect on the helix–loop–helix structure and calcium affinity and may be partly responsible for the difference in affinities between the high- and low-affinity sites in TnC. It has previously been proposed by Reid et al. (1981) that N-terminal helix formation is important for calcium binding, and the present work on 34-residue peptides reaffirms this hypothesis although it is unclear whether the residue at position 2 of the calcium-binding loop perturbs calcium binding through a helix–dipole or an $i$+4 electrostatic mechanism. In either case, however, the implication is that N-terminal helix formation appears to be a necessary requirement for calcium binding. Further, it has also been shown that single-site helix–loop–helix peptides can undergo an association to form a two-site domain (Shaw et al., 1990; Kay et al., 1991). In the calcium form of SCIII, numerous hydrophobic contacts are found at the interface of the N-terminal helix (helix E) and the C-terminal helix (helix F) of the symmetrically related helix–loop–helix partner (Shaw et al., 1990). This observation is similar to that in TnC where pairing of sites III and IV results in numerous hydrophobic contacts between helices E and H and between helices F and G (Herzberg & James, 1988; Satyshur et al., 1988), which act to stabilize the domain in the presence of calcium. This mechanism may be operating in the calcium-binding peptides studied here. In peptide LII, the amino acid substitution at position 2 may sufficiently alter the N-terminal helix in the presence of calcium so as not to allow helix–helix pairing as found in SCIII (Shaw et al., 1990) and possibly LIIL. This would suggest that there is a critical balance between the "loop" amino acid composition and its influence on the formation of adjacent $\alpha$-helices in the presence of calcium. Further studies are required in order to probe this dependence, which may be useful in the design of calcium-binding proteins and peptides with modified calcium affinities.

## Acknowledgments

We thank Robert Boyko for his assistance with the curve-fitting programs used, Paul Semchuk for his help in the synthesis and purification of the peptides, and Mike Nattriss for amino acid analysis. We are grateful to Sue Smith for typing the manuscript.

## References

Akke, M., & Forsen, S. (1990) *Proteins 8*, 23–29.
Allen, D. G., Blinks, J. R., & Prendergast, F. G. (1977) *Science 195*, 996–998.
Borin, G., Pezzoli, A., Marchiori, F., & Peggion, E. (1985) *Int. J. Pept. Protein Res. 26*, 528–538.
Borin, G., Ruzza, P., Rossi, M., Calderan, A., Marchiori, F., & Peggion, E. (1989) *Biopolymers 28*, 353–369.
Buchta, R., Bordi, E., & Fridkin, M. (1986) *Int. J. Pept. Protein Res. 28*, 289–297.
Bundi, A., & Wüthrich, K. (1979) *Biopolymers 18*, 285–298.
Chothia, C. H. (1974) *Nature 248*, 338–339.
Drabikowski, W., Brzeska, H., & Venyaminov, S. Y. (1982) *J. Biol. Chem. 257*, 11584–11590.
Drakenberg, T., Forsen, S., Thulin, E., & Vogel, H. J. (1987) *J. Biol. Chem. 262*, 672–678.
Gariépy, J., Sykes, B. D., Reid, R. E., & Hodges, R. S. (1982) *Biochemistry 21*, 1506–1512.
Ghadiri, M. R., & Choi, C. (1990) *J. Am. Chem. Soc. 112*, 1630–1632.
Golden, L. F., Corson, D. C., Sykes, B. D., Banville, D., & MacManus, J. P. (1989) *J. Biol. Chem. 264*, 20314–20319.
Goodman, M., Pechere, J. F., Haiech, J., & Demaille, J. G. (1979) *J. Mol. Evol. 13*, 331–352.
Guy, H. R. (1985) *Biophys. J. 47*, 61–70.
Hapak, R. C., Lammers, P. J., Palmisano, W. A., Birnbaum, E. R., & Henzl, M. T. (1989) *J. Biol. Chem. 264*, 18751–18760.
Herzberg, O., & James, M. N. G. (1988) *J. Mol. Biol. 203*, 761–779.
Hodges, R. S., Saund, A. K., Chog, P. C. S., St. Pierre, S. A., & Reid, R. E. (1981) *J. Biol. Chem. 256*, 1214–1224.
Hodges, R. S., Semchuk, P. D., Taneja, A. K., Kay, C. M., Parker, J. M. R., & Mant, C. L. (1988) *Pept. Res. 1*, 19–30.
Hofmann, T., Eng, S., Lilja, H., Drakenberg, T., Vogel, H., & Forsen, S. (1988) *Eur. J. Biochem. 172*, 307–313.
Hol, W. G. J. (1985) *Prog. Biophys. Mol. Biol. 48*, 149–195.
Hol, W. G. J., van Duijnen, P. T., & Berendsen, H. J. C. (1978) *Nature 273*, 443–446.
Hol, W. G. J., Halie, L. M., & Sander, C. (1981) *Nature 294*, 532–536.
Kanellis, P., Yang, J., Cheung, H. C., & Lenkinski, R. E. (1983) *Arch. Biochem. Biophys. 220*, 530–540.
Kretsinger, R. H., & Nockolds, C. E. (1973) *J. Biol. Chem. 248*, 3313–3326.
Kay, L. E., Forman-Kay, J. D., McCubbin, W. D., & Kay, C. M. (1991) *Biochemistry 30*, 4323–4333.
Leavis, P. C., Rosenfeld, S. S., Gergely, J., Grabarek, Z., & Drabikowski, W. (1978) *J. Biol. Chem. 253*, 5452–5459.
Linse, S., Brodin, P., Drakenberg, T., Thulin, E., Sellers, P., Elmden, K., Grundstrom, T., & Forsen, S. (1987) *Biochemistry 26*, 6723–6735.

Linse, S., Brodin, P., Johansson, C., Thulin, E., Grundstrom, T., & Forsen, S. (1988) *Nature 335*, 651–652.
MacManus, J. P., Hutrik, C. M. L., Sykes, B. D., Szabo, A. G., Williams, T. C., & Banville, D. (1989) *J. Biol. Chem. 264*, 3470–3477.
Malik, N. A., Anantharamaiah, G. M., Gawish, A., & Cheung, H. C. (1987) *Biochim. Biophys. Acta 911*, 221–230.
Marchiori, F., Borin, G., Chessa, G., Cavaggion, G., Michelin, L., & Peggion, E. (1983) *Hoppe-Seyler's Z. Physiol. Chem. 364*, 1019–1028.
Marqusee, S., & Baldwin, R. L. (1987) *Proc. Natl. Acad. Sci. U.S.A. 84*, 8898–8902.
Marsden, B. J., Hodges, R. S., & Sykes, B. D. (1988) *Biochemistry 27*, 4198–4206.
Marsden, B. J., Shaw, G. S., & Sykes, B. D. (1990) *Biochem. Cell Biol. 68*, 587–601.
Nagy, B., Potter, J. D., & Gergely, J. (1978) *J. Biol. Chem. 253*, 5971–5974.
Nicholson, H., Becktel, W. J., & Matthews, B. W. (1988) *Nature 336*, 651–656.
Palmisano, W. A., Trevino, C. L., & Henzl, M. T. (1990) *J. Biol. Chem. 265*, 14450–14456.
Pantoliano, M. W., Whitlow, M., Wood, J. F., Rollence, M. L., Finzel, B. C., Gillilard, G. L., Poulos, T. L., & Bryan, P. N. (1988) *Biochemistry 27*, 8311–8317.
Pantoliano, M. W., Whitlow, M., Wood, J. F., Dodd, S. W., Hardman, K. D., Rollence, M. L., & Bryan, P. N. (1989) *Biochemistry 28*, 7205–7213.
Potter, J. D., & Gergely, J. (1975) *J. Biol. Chem. 250*, 4628–4633.
Putkey, J. A., Sweeney, H. L., & Campbell, S. T. (1989) *J. Biol. Chem. 264*, 12370–12378.
Reid, R. E. (1987) *Int. J. Pept. Protein Res. 30*, 613–621.
Reid, R. E., & Hodges, R. S. (1980) *J. Theor. Biol. 84*, 401–444.
Reid, R. E., Gariépy, J., Saund, A. K., & Hodges, R. S. (1981) *J. Biol. Chem. 256*, 2742–2751.
Reinach, F. C., & Karlsson, R. (1988) *J. Biol. Chem. 263*, 2371–2376.
Satyshur, K. A., Rao, S. T., Pyzalska, D., Drendel, W., Greaser, M., & Sundaralingam, M. (1988) *J. Biol. Chem. 263*, 1628–1647.
Serpersu, E. H., Shortle, D., & Mildvan, A. S. (1987) *Biochemistry 26*, 1289–1300.
Shaw, G. S., Hodges, R. S., & Sykes, B. D. (1990) *Science 249*, 280–283.
Shaw, G. S., Golden, L. F., Hodges, R. S., & Sykes, B. D. (1991) *J. Am. Chem. Soc.* (in press).
Shoemaker, K. R., Kim, P. S., York, E. J., Stewart, J. M., & Baldwin, R. L. (1987) *Nature 326*, 563–567.
Strynadka, N. C. J., & James, M. N. G. (1989) *Annu. Rev. Biochem. 58*, 951–998.
Tsuda, S., Hasegawa, Y., Yoshida, M., Yagi, K., & Hikichi, K. (1988) *Biochemistry 27*, 4120–4126.
Tsuji, T., & Kaiser, E. T. (1991) *Proteins 9*, 12–22.
Williams, T. C., Shelling, J. G., & Sykes, B. D. (1985) in *NMR in the Life Sciences* (Bradbury, E. M., & Nicolini, C., Eds.) pp 93–103, Plenum Press, New York.
Williams, T. C., Corson, D. C., Oikawa, K., McCubbin, W. D., Kay, C. M., & Sykes, B. D. (1986) *Biochemistry 25*, 1835–1846.

# Rotation and Interactions of Genetically Expressed Cytochrome P-450IA1 and NADPH–Cytochrome P-450 Reductase in Yeast Microsomes†

Tadashi Iwase,‡ Toshiyuki Sakaki,§ Yoshiyasu Yabusaki,§ Hideo Ohkawa,§ Yoshihiro Ohta,‡ and Suguru Kawato*,‡
*Institute of Physics, College of Arts and Sciences, University of Tokyo at Komaba, Meguro, Tokyo 153, Japan, and Biotechnology Laboratory, Takarazuka Research Center, Sumitomo Chemical Company, Ltd., Takarazuka, Hyogo 665, Japan*
*Received March 19, 1991; Revised Manuscript Received May 28, 1991*

ABSTRACT: Rat liver cytochrome P-450IA1 and/or yeast NADPH–cytochrome P-450 reductase was expressed genetically in yeast microsomes. The ratio of P-450IA1 to the reductase was about 17:1 and 1:2 without and with coexpression of the reductase, respectively. Rotational diffusion of P-450IA1 was examined by observing the flash-induced absorption anisotropy, $r(t)$, of the heme·CO complex. In only P-450IA1-expressed microsomes, 28% of P-450IA1 was rotating with a rotational relaxation time ($\phi$) of about 1200 $\mu$s. The mobile population was increased to 43% by the presence of the coexpressed reductase, while $\phi$ was not changed significantly. Increased concentration of KCl from 0 to 1000 mM caused considerable mobilization of P-450IA1. The results demonstrate a proper incorporation of P-450IA1 molecules into yeast microsomal membranes. The significant mobilization of P-450IA1 by the presence of reductase suggests a possible transient association of P-450IA1 with the reductase.

Cytochrome P-450 and NADPH–cytochrome P-450 reductase are key enzymes in the hepatic microsomal monooxygenase system, catalyzing the oxidative metabolism of various drugs and xenobiotics as well as endogenous substrates (Estabrook et al., 1979; White & Coon, 1980). Among numerous isozymes of P-450, extensive evidence exists that particularly the methylcholanthrene-induced cytochrome P-450IA1 converts polycyclic aromatic hydrocarbons to highly carcinogenic compounds (Harada & Omura, 1981; Guengerich, 1987). Electron-transfer mechanisms from the reductase to cytochrome P-450IA1[1] were not established so far. Es-

† This work was supported by grants from the Ministry of Education, Science and Culture of Japan (to S.K.) and by the Research and Development Projects of Basic Technologies for Future Industries from NEDO (New Energy and Industrial Technology Development Organization) (to H.O.).
* To whom correspondence should be addressed.
‡ University of Tokyo at Komaba.
§ Sumitomo Chemical Co., Ltd.

0006-2960/91/0430-8347$02.50/0 